

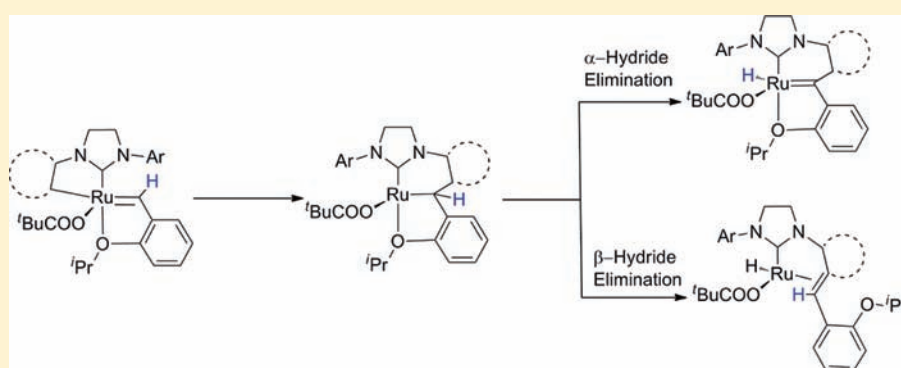
Decomposition Pathways of Z-Selective Ruthenium Metathesis Catalysts

Myles B. Herbert,[†] Yu Lan,[‡] Benjamin K. Keitz,[†] Peng Liu,[‡] Koji Endo,[†] Michael W. Day,^{†,§} K. N. Houk,^{*,‡} and Robert H. Grubbs^{*,†}

[†]Arnold and Mabel Beckman Laboratory of Chemical Synthesis, Division of Chemistry and Chemical Engineering, California Institute of Technology, Pasadena, California 91125, United States

[‡]Department of Chemistry and Biochemistry, University of California, Los Angeles, California 90095-1569, United States

S Supporting Information



ABSTRACT: The decomposition of a Z-selective ruthenium metathesis catalyst and structurally similar analogues has been investigated utilizing X-ray crystallography and density functional theory. Isolated X-ray crystal structures suggest that recently reported C–H activated catalysts undergo decomposition via insertion of the alkylidene moiety into the chelating ruthenium–carbon bond followed by hydride elimination, which is supported by theoretical calculations. The resulting ruthenium hydride intermediates have been implicated in previously observed olefin migration, and thus lead to unwanted byproducts in cross metathesis reactions. Preventing these decomposition modes will be essential in the design of more active and selective Z-selective catalysts.

INTRODUCTION

Olefin metathesis has gained increasing popularity as an efficient and effective method for the construction of carbon–carbon bonds.¹ The development of a variety of well-defined transition metal catalysts, particularly functional group tolerant ruthenium-based complexes, has allowed for the widespread use of this methodology for a variety of applications, including natural product synthesis,² breakdown of olefinic biomolecules by ethenolysis,³ and materials chemistry.⁴ We recently reported on the synthesis and reactivity of **1**, a C–H activated catalyst containing a five-membered chelating N-heterocyclic carbene (NHC) ligand (Scheme 1).⁵ Its unprecedented ability to preferentially form the thermodynamically disfavored Z-isomer in cross metathesis (CM) reactions has stimulated research into such C–H activated architectures.

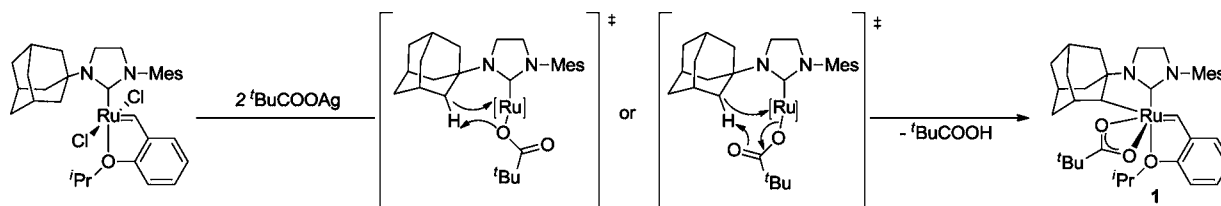
For **1**, the initial C–H activation event has been proposed to proceed via a four- or six-membered transition state between an alkyl carbon–hydrogen bond on the N-adamantyl substituent of the NHC, and a ruthenium-bound carboxylate ligand (Scheme 1).^{5a} Carboxylate-driven C–H bond activations of this type have been studied for a variety of late transition metal

complexes.⁶ With this mode of activation, a carbon–metal bond is formed with concurrent generation of the corresponding carboxylic acid. In contrast, previous generations of ruthenium metathesis catalysts have been proposed to decompose upon C–H activation by oxidative addition. This oxidative addition process produces a ruthenium hydride that readily inserts into the alkylidene and diminishes catalytic activity.^{7a} The unique nature of the carboxylate-driven mechanism allows for isolation of metathesis active C–H activated complexes without the accompanying formation of a ruthenium hydride.

A thorough understanding of decomposition pathways is important for designing more efficient and improved catalysts.⁷ Research investigating the decomposition of metathesis catalysts has led to the rational design of more stable and active species with ligands chosen to reduce the prevalence of undesired side reactions. For example, backbone substitution was introduced into the NHC ligands of ruthenium catalysts to restrict N-aryl rotation that leads to the aforementioned

Received: February 2, 2012

Published: April 13, 2012

Scheme 1. Synthesis of C–H Activated Catalyst **1** with Proposed Transition States for C–H Activation^a

^aMes = 2,4,6-trimethylphenyl.

decomposition by oxidative addition.⁸ Known decomposition products of metathesis catalysts cause olefin migration of alkene substrates, as well as other side reactions;⁹ such migration has been observed in our studies on the *Z*-selective homocoupling of terminal olefins.^{5b,c} Computational studies have provided important insights into several decomposition mechanisms involving previous generations of ruthenium metathesis catalysts, including alkylidene insertion into the *ortho* C–H bond of an *N*-aryl substituent,^{7e,h} β -hydride elimination from a ruthenacyclobutane intermediate,⁷ⁱ and decomposition induced by coordination of CO.^{7g} We thus sought to design more selective and stable analogues of catalyst **1** by investigating the decomposition of **1** and its analogues. Herein, we report on several unique decomposition structures and their mechanisms of formation. To support our mechanisms, density functional theory (DFT) calculations were performed to investigate the proposed decomposition pathways of the C–H activated catalyst **1**.

RESULTS AND DISCUSSION

Catalyst **1** was exposed to an excess of CO gas at $-78\text{ }^{\circ}\text{C}$ in an effort to promote a (1,1)-insertion of a bound CO ligand into the ruthenium–carbon bond of the chelated NHC to yield a novel chelated catalyst architecture with an intact alkylidene. However, decomposition of the alkylidene moiety was observed, and crystallographic analysis revealed formation of **2** (Figure 1), an alkyl ruthenium complex saturated with CO ligands and showing covalent attachment of the *N*-adamantyl substituent to the former alkylidene carbon (Scheme 2). Ligand substitution by the π -acidic CO ligands decreased the ability of the metal center to stabilize the alkylidene carbon by back bonding. This destabilization was presumably relieved by insertion of the alkylidene into the ruthenium–carbon bond

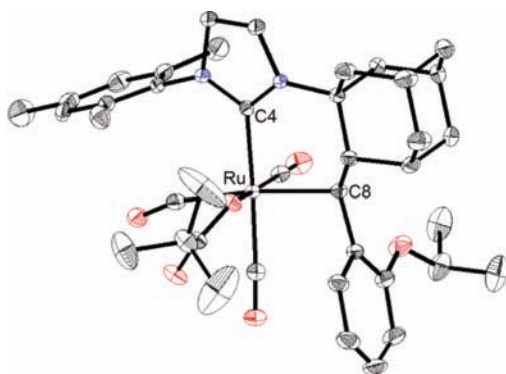
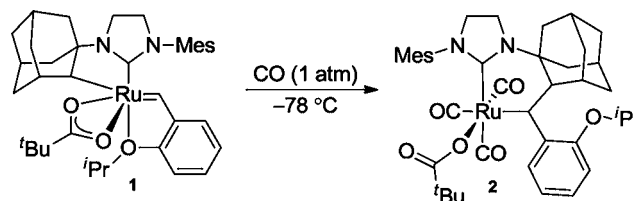


Figure 1. X-ray crystal structure of **2**. Displacement ellipsoids are drawn at 50% probability. For clarity, hydrogen atoms have been omitted. Selected bond lengths (Å) for **2**: C4–Ru 2.107, C8–Ru 2.195.

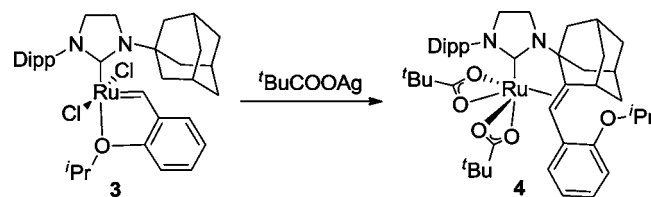
Scheme 2. Decomposition Product **2** Derived from Exposure of **1** to Excess CO



to form complex **2**.¹⁰ It was subsequently proposed that this alkylidene insertion phenomenon could be common for C–H activated catalysts in the absence of CO, and that ruthenium–alkyl complexes analogous to **2** could undergo hydride elimination reactions when not saturated with CO ligands, leading to complexes incapable of productive metathesis.

Indeed, we were able to isolate a unique decomposition product resulting from alkylidene insertion (as with **2**) and subsequent β -hydride elimination when C–H activation was attempted with catalyst **3** (Scheme 3).¹¹ Treating complex **3**

Scheme 3. Decomposition Product **4** Derived from Exposure of **3** to ^tBuCOOAg^a



^aDipp = 2,6-diisopropylphenyl.

with silver pivalate (^tBuCOOAg) resulted in the expected ligand exchange of chlorides for pivalates, and concomitant generation of silver(I) chloride. Monitoring the reaction of **3** by ¹H NMR spectroscopy revealed the initial formation of a monocarboxylate, monochloride ruthenium alkylidene species that slowly disappeared with the appearance of pivalic acid. A C–H activated species was subsequently observed but was metastable, slowly converting to a ruthenium hydride as observed by ¹H NMR. X-ray crystal analysis of the resulting decomposition product revealed the novel η^2 -bound olefin ruthenium complex **4** (Figure 2). Generation of pivalic acid suggested that C–H activation of the *N*-adamantyl substituent had occurred but that the complex rapidly decomposed by a process involving alkylidene insertion and β -hydride elimination, as evidenced by the formation of a ruthenium hydride and the η^2 -bound olefin motif in the X-ray crystal structure of **4**. The formation of a ruthenium hydride via β -hydride elimination is further supported by observed olefin migration in cross metathesis reactions.^{5b,c}

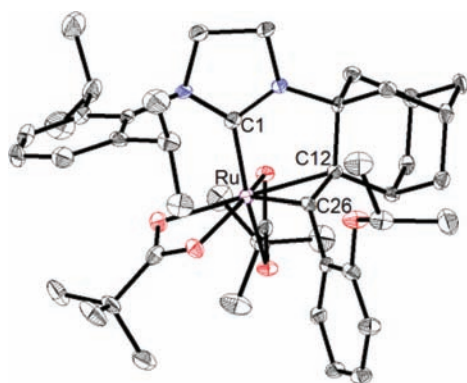
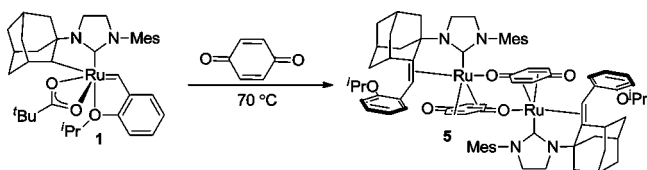


Figure 2. X-ray crystal structure of **4**. Displacement ellipsoids are drawn at 50% probability. For clarity, hydrogen atoms have been omitted. Selected bond lengths (Å) for **4**: C1–Ru 1.944, C12–Ru 2.130, C26–Ru 2.102, C12–C26 1.434.

Further evidence for β -hydride elimination playing a role in the decomposition of C–H activated catalysts was uncovered by treating catalyst **1** with *p*-benzoquinone (Scheme 4).¹²

Scheme 4. Decomposition Product 5 Derived from Exposure of 1 to Excess *p*-Benzoquinone



Addition of this additive to **1** in C_6D_6 led to an immediate color change from purple to red/orange and decomposition of the original complex as evidenced by the disappearance of the alkylidene resonance in the 1H NMR spectrum. Crystals of the decomposition structure (**5**) were obtained, and analysis by X-ray diffraction revealed the structure to be a ruthenium(0) dimer bridged by two benzoquinone ligands along with η^2 -bound olefin motifs (Figure 3), a binding mode also observed for complex **4**.

The olefins of the benzoquinone ligands in **5** appear to be coordinated primarily in an η^4 fashion as demonstrated by the downfield ^{13}C carbonyl resonance (CD_2Cl_2 , $\delta = 211.5$ ppm), the relatively long C–O bond length (1.27 Å), and the boat-like conformation of the benzoquinone ligands.¹³ Complexes similar to **5** have previously been observed for ruthenium¹³ and other metals,¹⁴ although they are typically formed by simple ligand displacement. This novel structure appears to be the result of alkylidene insertion (as observed for complex **2**) and subsequent β -hydride elimination (as observed for **4**), reduction, and dimerization.

We next turned our attention to the synthesis of analogues of catalyst **1** with stronger ruthenium–carbon bonds derived from C–H activation of an sp^2 -hybridized carbon–hydrogen bond,¹⁵ and observed a unique decomposition mode seemingly resulting from alkylidene insertion and α -hydride elimination (Scheme 5). Complex **6**, a species containing hydrogen atoms at the *ortho*-position of its *N*-aryl substituents, immediately decomposed upon treatment with tBuCOOAg , with the appearance of pivalic acid and the disappearance of the starting material's alkylidene proton resonance. The resulting decomposition product (**8**) was crystallographically characterized, and

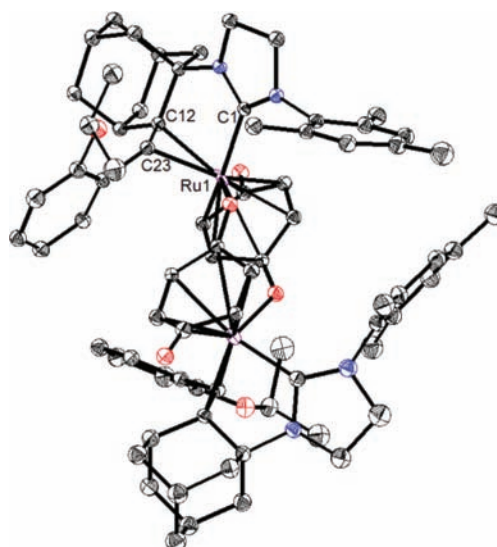
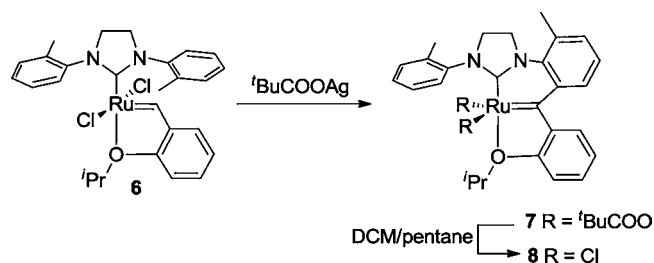


Figure 3. X-ray crystal structure of **5**. Displacement ellipsoids are drawn at 50% probability. For clarity, hydrogen atoms have been omitted. Selected bond lengths (Å) for **5**: C1–Ru1 2.061, C12–Ru1 2.245, C23–Ru1 2.168, C12–C23 1.418.

Scheme 5. Decomposition Products 7 and 8 Derived from Exposure of 6 to tBuCOOAg



its structure revealed attachment of the benzylidene carbon to the *ortho* carbon of the *N*-aryl group, with retention of the alkylidene moiety (Figure 4).¹⁶ Although mass spectrometry data of the initial product mixture suggested formation of **7**, upon prolonged treatment with a mixture of methylene

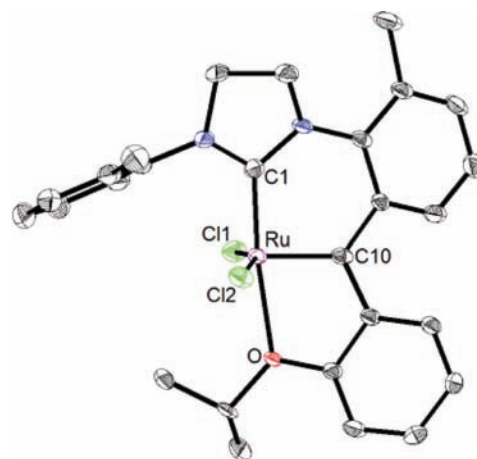


Figure 4. X-ray crystal structure of **8**. Displacement ellipsoids are drawn at 50% probability. For clarity, hydrogen atoms have been omitted. Selected bond lengths (Å) for **8**: C1–Ru 1.913, C10–Ru 1.829, Cl1–Ru 2.340, Cl2–Ru 2.341.

Scheme 6. Proposed Decomposition Pathways for C–H Activated Ruthenium Metathesis Catalysts

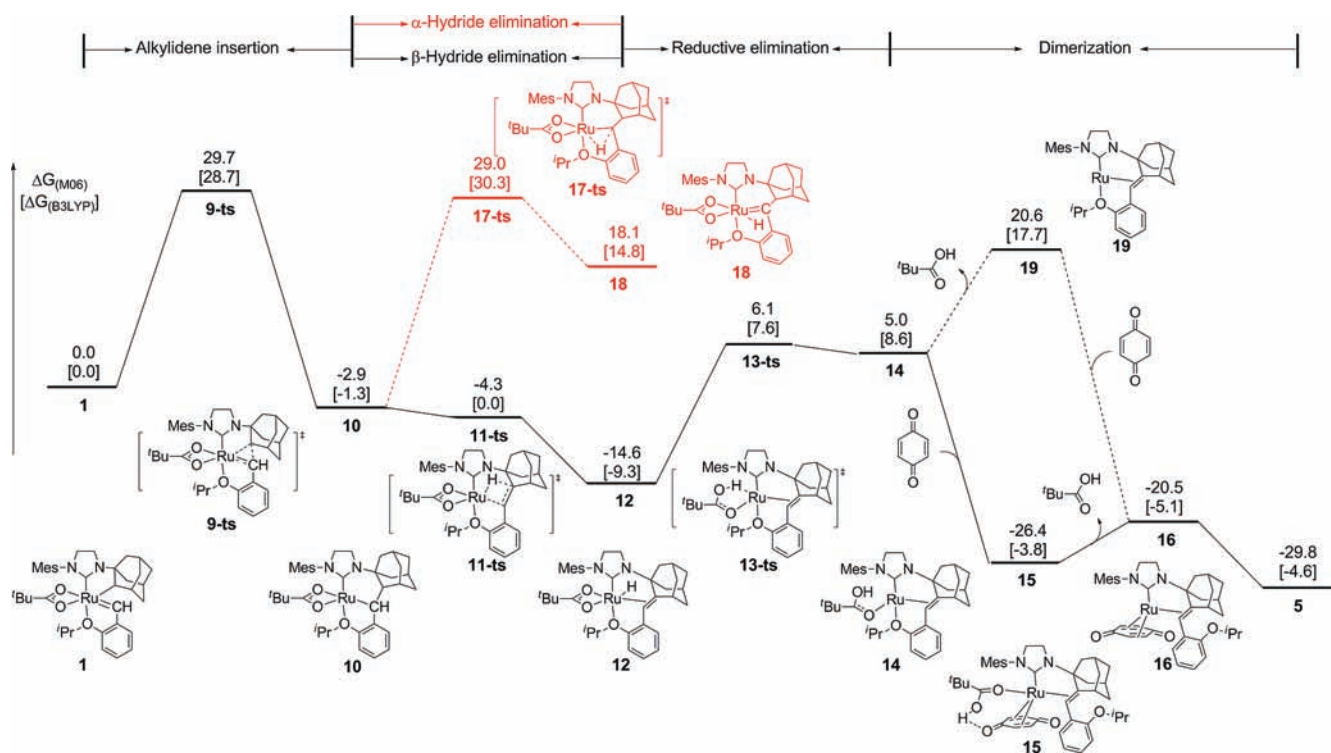
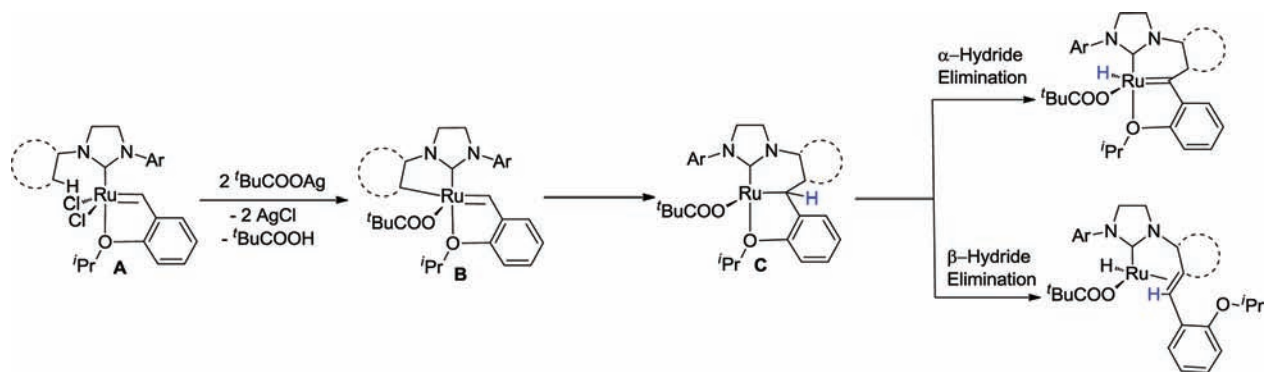


Figure 5. The free energy profile of the decomposition pathways for C–H activated ruthenium catalyst **1**. The values are relative free energies calculated by M06 and B3LYP (in square brackets) and are given in kcal/mol. B3LYP was used in the geometry optimizations.

chloride and pentane, the pivalate ligands were replaced by chlorides derived from the chlorinated solvent to yield **8**.¹⁷ Observation of pivalic acid again suggested that a C–H activation event had occurred but with subsequent decomposition. Attempted C–H activation of various complexes containing *N*-aryl groups with unsubstituted *ortho* positions resulted in this decomposition mode.

From the complexes presented above, we were able to elucidate a general decomposition mechanism for species related to complex **1** (Scheme 6). It is proposed that the unactivated catalysts **3** and **6**, upon treatment with ^tBuCOOAg, form chelated architectures with an intact ruthenium alkydine (**B**), as observed for catalyst **1**. However, these C–H activated species react further, as the alkydine inserts into the newly formed ruthenium–carbon bond to yield alkyl ruthenium intermediate **C**. The isolated structure of complex **2** provides evidence for the in situ formation of this alkyl intermediate. Following insertion, the complex can undergo α - or β -hydride

elimination to regenerate an alkydine (as in **7** and **8**) or form an η^2 -bound olefin complex (as in **4** and **5**), respectively.

In an effort to support our proposed mechanism, we performed DFT calculations on the decomposition modes of C–H activated catalyst **1**. Both α - and β -hydride elimination pathways were investigated, and the free energy profile is shown in Figure 5. Energies were calculated in the gas phase using M06 and with a mixed basis set of SDD for ruthenium and 6-311+G(d,p) for other atoms; B3LYP energies are also given in Figure 5. Geometries were optimized with B3LYP/LANL2DZ-6-31G(d), and all calculations were performed with Gaussian 09.¹⁸ On the basis of computational results, we report that the decomposition of C–H activated catalysts initiates by alkydine insertion into the chelating ruthenium–carbon bond as proposed.

The decomposition of catalyst **1** initiates via insertion of the alkydine into the ruthenium–carbon (adamantyl) bond (**9-ts**), for which both M06 and B3LYP predicted an activation barrier of ~ 29 kcal/mol. The alkydine insertion leads to alkyl

ruthenium complex **10**, a structure similar to the proposed intermediate **C** in Scheme 6. β -Hydride elimination from **10** is facile (**11-ts**),¹⁹ while the activation barrier for α -hydride elimination (**17-ts**) is calculated to be 33.3 kcal/mol higher. This β -hydride elimination reaction leads to ruthenium hydride intermediate **12**, which is 14.6 kcal/mol more stable than catalyst **1**. This energy difference agrees well with previous experimental observations of ruthenium–hydride species by ¹H NMR. The overall exergonicity of the transformation from **1** to **12** suggests that the alkylidene insertion is irreversible.

The preference for β -hydride elimination over α -hydride elimination agrees with the observed decomposition product derived from complex **3** (Scheme 3). Previous experimental and theoretical studies performed on hydride elimination reactions of ruthenium pincer-type complexes analogous to intermediate **C** also suggest that when α - and β -hydrogens are both present, β -hydride elimination is energetically favored; however, when the molecule lacks β -hydrogens, α -hydride elimination occurs.²⁰ This is the case for the alkyl intermediate (**C**) of complex **6** resulting from C–H activation and alkylidene insertion, as its backbone does not contain β -hydrogens, and thus only α -hydride elimination is observed. The ruthenium–hydride species (analogues of **12** and **18**) generated from these hydride elimination reactions subsequently react with the excess ^tBuCOOAg to generate **4** and **7**, respectively.²¹

The transformation from **12** to the dimeric complex **5** was also investigated using DFT, and the free energy profile is shown in Figure 5. Reductive elimination of pivalic acid from ruthenium hydride **12** forms a ruthenium(0) complex **14**, which is 19.6 kcal/mol less stable than complex **12**.²² Subsequent ligand exchange replaces the pivalic acid with benzoquinone and forms the ruthenium(0) complex **16**, in which the benzoquinone is η^4 -coordinated with ruthenium; the benzoquinone binds to the ruthenium much more strongly than pivalic acid. M06 predicted that the ruthenium(0)–benzoquinone complex **16** is 25.5 kcal/mol more stable than the ruthenium(0)–pivalic acid complex **14**, while B3LYP predicted that **16** is only 13.7 kcal/mol more stable than **14**. The energy differences between B3LYP and M06 here are not unexpected, because B3LYP is known to underestimate the binding energy of olefins to ruthenium centers.²³ The ligand exchange from **14** to **16** occurs via an associative pathway involving complex **15**, as the dissociative ligand exchange pathway would involve the unstable 14 electron complex **19** and thus is predicted to be less favorable. The electron-deficient C=C bonds in *p*-benzoquinone bind strongly with the π -basic zerovalent ruthenium in complexes **15** and **16**.²⁴ Dimerization of complex **16** leads to the crystallographically characterized ruthenium dimer complex **5** and is exergonic by 9.4 kcal/mol. Addition of benzoquinone facilitates the decomposition of ruthenium hydride **12** by stabilizing the ruthenium(0) species that leads to formation of the stable dimeric complex **5**. The increased decomposition rate with addition of benzoquinone suggests that this additive may also accelerate alkylidene insertion (**9-ts**); however, the mechanism of this process is not clear.

CONCLUSION

We have investigated the decomposition of a new class of *Z*-selective metathesis catalysts with chelating NHC ligands resulting from an initial carboxylate-driven C–H bond insertion. Formation of a stable carbon–ruthenium bond in the presence of an alkylidene seems to be subtly dependent on

a variety of steric and electronic factors. A number of decomposition products derived from side reactions of C–H inserted complexes were characterized by X-ray crystallography, and, from these, decomposition pathways were proposed. The decomposition of C–H activated catalysts is thought to proceed via insertion of the alkylidene into the chelating ruthenium–carbon bond to yield an alkyl ruthenium intermediate. Because of the presence of a vacant coordination site, subsequent hydride elimination can occur to these alkyl intermediates to generate a ruthenium hydride, which has been proposed to cause olefin migration for alkene substrates. Density functional calculations were performed and support the proposed decomposition pathway of **1**, which proceeds via insertion of the alkylidene into the chelating ruthenium–carbon bond and subsequent β -hydride elimination, leading to a ruthenium hydride complex.

The decomposition modes presented above are markedly distinct from those observed for previous generations of ruthenium metathesis catalysts. Preventing alkylidene insertion and hydride elimination will be key criteria in future catalyst development. Despite these decomposition modes, such chelated complexes have proven to be effective catalysts for *Z*-selective olefin metathesis. Because decomposition can reduce overall catalyst activity and enable undesired side reactions, designing more stable catalysts by understanding catalyst decomposition is essential for highly chemoselective metathesis reactions.

ASSOCIATED CONTENT

Supporting Information

Experimental details, NMR spectra, crystallographic data, optimized Cartesian coordinates and energies, and complete ref 18. This material is available free of charge via the Internet at <http://pubs.acs.org>.

AUTHOR INFORMATION

Corresponding Author

rhg@caltech.edu; hok@chem.ucla.edu

Notes

The authors declare no competing financial interest.

[§]Deceased January 27, 2012.

ACKNOWLEDGMENTS

This work is dedicated to the memory of Dr. Michael W. Day. Dr. David VanderVelde is thanked for his assistance with NMR characterization and experiments. Lawrence Henling is acknowledged for X-ray crystallographic analysis. This work was financially supported by the NIH (NIH 5R01GM031332-27, R.H.G.), the NSF (CHE-1048404, R.H.G. and CHE-1059084, K.N.H.), Mitsui Chemicals, Inc. (K.E.), and the NDSEG (fellowship to B.K.K.). The Bruker KAPPA APEXII X-ray diffractometer was purchased via an NSF CRIF:MU award to the California Institute of Technology (CHE-0639094). Materia, Inc. is acknowledged for its generous donation of metathesis catalysts. Calculations were performed on the Hoffman2 cluster at UCLA and the Extreme Science and Engineering Discovery Environment (XSEDE), which is supported by the National Science Foundation (OCI-1053575).

REFERENCES

- (1) (a) Fürstner, A. *Angew. Chem., Int. Ed.* **2000**, *39*, 3013. (b) Trnka, T. M.; Grubbs, R. H. *Acc. Chem. Res.* **2001**, *34*, 18. (c) Schrock, R. R. *Chem. Rev.* **2002**, *102*, 145. (d) Schrock, R. R.; Hoveyda, A. H. *Angew. Chem., Int. Ed.* **2003**, *42*, 4592. (e) Vougioukalakis, G.; Grubbs, R. H. *Chem. Rev.* **2009**, *110*, 1746. (f) Samojłowicz, C.; Bieniek, M.; Grela, K. *Chem. Rev.* **2009**, *109*, 3708.
- (2) (a) Cossy, J.; Arseniyadis, S.; Meyer, C. *Metathesis in Natural Product Synthesis: Strategies, Substrates, and Catalysts*, 1st ed.; Wiley-VCH: Weinheim, 2010. (b) Meek, S. J.; O'Brien, R. V.; Llaveria, J.; Schrock, R. R.; Hoveyda, A. H. *Nature* **2011**, *471*, 461. (c) Yu, M.; Wang, C.; Kyle, A. F.; Jakubec, P.; Dixon, D. J.; Schrock, R. R.; Hoveyda, E. H. *Nature* **2011**, *479*, 88.
- (3) (a) Thomas, R. M.; Keitz, B. K.; Champagne, T. M.; Grubbs, R. H. *J. Am. Chem. Soc.* **2011**, *133*, 7490. (b) Marinescu, S. C.; Schrock, R. R.; Muller, P.; Hoveyda, A. H. *J. Am. Chem. Soc.* **2009**, *131*, 10840.
- (4) (a) Leitgeb, A.; Wappel, J.; Slugovc, C. *Polymer* **2010**, *51*, 2927. (b) Liu, X.; Basu, A. *J. Organomet. Chem.* **2006**, *691*, 5148. (c) Xia, Y.; Verduzco, R.; Grubbs, R. H.; Kornfield, J. A. *J. Am. Chem. Soc.* **2008**, *130*, 1735.
- (5) (a) Endo, K.; Grubbs, R. H. *J. Am. Chem. Soc.* **2011**, *133*, 8525. (b) Keitz, B. K.; Endo, K.; Herbert, M. B.; Grubbs, R. H. *J. Am. Chem. Soc.* **2011**, *133*, 9686. (c) Keitz, B. K.; Endo, K.; Patel, P. R.; Herbert, M. B.; Grubbs, R. H. *J. Am. Chem. Soc.* **2012**, *134*, 693.
- (6) (a) Davies, D. L.; Donald, S. M. A.; Macgregor, S. A. *J. Am. Chem. Soc.* **2005**, *127*, 13754. (b) Davies, D. L.; Donald, S. M. A.; Al-Duaij, O.; Macgregor, S. A.; Pölleth, M. *J. Am. Chem. Soc.* **2006**, *128*, 4210. (c) Ess, D. H.; Bischof, S. M.; Oxgaard, J.; Periana, R. A.; Goddard, W. A. *Organometallics* **2008**, *27*, 6440. (d) Boutadla, Y.; Davies, D. L.; Macgregor, S. A.; Polador-Bahamonde, A. I. *Dalton Trans.* **2009**, 5820. (e) Tsurugi, H.; Fujita, S.; Choi, G.; Yamagata, T.; Ito, S.; Miyasaka, H.; Mashima, K. *Organometallics* **2010**, *29*, 4120.
- (7) (a) Hong, S. H.; Chlenov, A.; Day, M. W.; Grubbs, R. H. *Angew. Chem., Int. Ed.* **2007**, *46*, 5148. (b) Hong, S. H.; Day, M. W.; Grubbs, R. H. *J. Am. Chem. Soc.* **2004**, *126*, 7414. (c) Hong, S. H.; Wenzel, A. G.; Salguero, T. T.; Day, M. W.; Grubbs, R. H. *J. Am. Chem. Soc.* **2007**, *129*, 7961. (d) Vehlow, K.; Gessler, S.; Blechert, S. *Angew. Chem., Int. Ed.* **2007**, *46*, 8082. (e) Leitao, E. M.; Dubberley, S. R.; Piers, W. E.; Wu, Q.; McDonald, R. *Chem.-Eur. J.* **2008**, *14*, 11565. (f) Poater, A.; Cavallo, L. *J. Mol. Catal. A: Chem.* **2010**, *324*, 75. (g) Poater, A.; Ragone, F.; Correa, A.; Cavallo, L. *J. Am. Chem. Soc.* **2009**, *131*, 9000. (h) Mathew, J.; Koga, N.; Suresh, C. H. *Organometallics* **2008**, *27*, 4666. (i) Rensburg, W. J.; Steynberg, P. J.; Meyer, W. H.; Kirk, M. M.; Forman, G. S. *J. Am. Chem. Soc.* **2004**, *126*, 14332.
- (8) (a) Chung, C. K.; Grubbs, R. H. *Org. Lett.* **2008**, *10*, 2693. (b) Kuhn, K. M.; Bourg, J.; Chung, C. K.; Virgil, S. C.; Grubbs, R. H. *J. Am. Chem. Soc.* **2009**, *131*, 5313. (c) Ragone, F.; Poater, A.; Cavallo, L. *J. Am. Chem. Soc.* **2010**, *132*, 4249. (d) Poater, A.; Bahri-Laleh, N.; Cavallo, L. *Chem. Commun.* **2011**, *47*, 6674.
- (9) (a) Courchay, F. C.; Sworen, J. C.; Ghiviriga, I.; Abboud, K. A.; Wagener, K. B. *Organometallics* **2006**, *25*, 6074. (b) Schmidt, B. *Eur. J. Org. Chem.* **2004**, *9*, 1865. (c) Camm, K. D.; Castro, N. M.; Liu, W.; Czechura, P.; Snelgrove, J. L.; Fogg, D. E. *J. Am. Chem. Soc.* **2007**, *129*, 4168.
- (10) For a discussion of CO-induced insertion reactions of ruthenium alkylidenes, see: Weng, W.; Parkin, S.; Ozerov, O. V. *Organometallics* **2006**, *25*, 5345.
- (11) Research on previous generations of ruthenium metathesis catalysts has revealed that increasing the steric bulk of an *N*-aryl groups can lead to increased activity and stability: (a) Dinger, M. B.; Mol, J. C. *Adv. Synth. Catal.* **2002**, *344*, 671. (b) Ritter, T.; Hejl, A.; Wenzel, A. G.; Funk, T. W.; Grubbs, R. H. *Organometallics* **2006**, *25*, 5740. (c) Fürstner, A.; Ackermann, L.; Gabor, B.; Goddard, R.; Lehmann, C. W.; Mynott, R.; Stelzer, F.; Thiel, O. R. *Chem.-Eur. J.* **2001**, *7*, 3236.
- (12) *p*-Benzoquinone is an additive shown to prevent olefin migration. For a reference, see: Hong, S. H.; Sanders, D. P.; Lee, C. W.; Grubbs, R. H. *J. Am. Chem. Soc.* **2005**, *127*, 17160.
- (13) (a) Takao, T.; Akiyoshi, K.; Suzuki, H. *Organometallics* **2008**, *27*, 4199–4206. (b) Ura, Y.; Sato, Y.; Shiotsuki, M.; Suzuki, T.; Wada, K.; Kondo, T.; Mitsudo, T.-a. *Organometallics* **2003**, *22*, 77–82. (c) Barral, M. C.; González-Prieto, R.; Jiménez-Aparicio, R.; Priego, J. L.; Torres, M. R.; Urbanos, F. A. *Inorg. Chim. Acta* **2005**, *358*, 217–221. (d) Kumbhakar, D.; Sarkar, B.; Maji, S.; Mobin, S. M.; Fiedler, J.; Urbanos, F. A.; Jiménez-Aparicio, R.; Kaim, W.; Lahiri, G. K. *J. Am. Chem. Soc.* **2008**, *130*, 17575–83.
- (14) (a) Moussa, J.; Amouri, H. *Angew. Chem., Int. Ed.* **2008**, *47*, 1372–80. (b) Moussa, J.; Guyard-Duhayon, C.; Herson, P.; Amouri, H.; Rager, M. N.; Jutand, A. *Organometallics* **2004**, *23*, 6231–6238.
- (15) Siegbahn, E. M. *J. Phys. Chem.* **1995**, *99*, 12723.
- (16) A structurally similar decomposition product has been reported for catalysts containing *N*-phenyl groups, wherein decomposition was thought to proceed through pericyclic cyclization and oxidation by O₂ (see ref 7d). This postulated mechanism of decomposition does not account for any carboxylate-driven C–H activation events and cannot proceed in an O₂-free environment; thus, we expected a different decomposition mechanism to yield **7** and **8**.
- (17) Reactions of methylene chloride with ruthenium complexes to produce metal chloride bonds have been reported: (a) Oliván, M.; Caulton, K. G. *Inorg. Chem.* **1999**, *38*, 566. (b) Pechtl, M. H. G.; Ben-David, Y.; Giunta, D.; Busch, S.; Taniguchi, Y.; Wisniewski, W.; Görls, H.; Mynott, R. J.; Theyssen, N.; Milstein, D.; Leitner, W. *Chem.-Eur. J.* **2007**, *13*, 1539.
- (18) Frisch, M. J.; et al. *Gaussian 09*, revision B.01; Gaussian, Inc.: Wallingford, CT, 2010. See the Supporting Information for more details of the computational methods.
- (19) Both B3LYP and M06 predicted very low barriers for β -hydride elimination. B3LYP predicted the barrier from **10** to **11-ts** to be 1.3 kcal/mol. M06 single point calculations with B3LYP geometries resulted in a small negative barrier, due to the different locations of saddle point on M06 and B3LYP surfaces.
- (20) (a) Kuznetsov, V. F.; Abdur-Rashid, K.; Lough, A. J.; Gusev, D. G. *J. Am. Chem. Soc.* **2006**, *128*, 14388. (b) Leis, W.; Mayer, H. A.; Kaska, W. C. *Coord. Chem. Rev.* **2008**, *252*, 1787.
- (21) It is proposed that these ruthenium hydrides react with ^tBuCOOAg to produce an ill-defined mixture of silver(I) hydrides. All attempts to observe such species by ¹H NMR were unsuccessful due to insolubility of the resulting gray precipitate in deuterated solvents.
- (22) Pivalic acid generation is observed by ¹H NMR after the addition of *p*-benzoquinone to **1**.
- (23) (a) Kulkarni, A. D.; Truhlar, D. G. *J. Chem. Theory Comput.* **2011**, *7*, 2325. (b) Handzlik, J.; Sliwa, P. *Chem. Phys. Lett.* **2010**, *493*, 273. (c) Torker, S.; Merki, D.; Chen, P. *J. Am. Chem. Soc.* **2008**, *130*, 4808. (d) Zhao, Y.; Truhlar, D. G. *Org. Lett.* **2007**, *9*, 1967.
- (24) Johnson, J. B.; Rovis, T. *Angew. Chem., Int. Ed.* **2008**, *47*, 840.